Published in final edited form as:
J Proteome Res. 2008 November ; 7(11): 4914–4925. doi:10.1021/pr800574c.

Characterization of the Human COP9 Signalosome Complex Using Affinity Purification and Mass Spectrometry

Lei Fang[†], **Xiaorong Wang**[†], **Kosj Yamoah**[‡], **Phang-lang Chen**[§], **Zhen-Qiang Pan**[‡], and **Lan Huang**[*,†]

Departments of Physiology & Biophysics and Developmental & Cell Biology, University of California, Irvine, California 92697, Department of Oncological Sciences, Mount Sinai School of Medicine, New York, New York 10029, and Department of Biological Chemistry, University of California, Irvine, California 92697

Abstract

The COP9 signalosome (CSN) is a multiprotein complex that plays a critical role in diverse cellular and developmental processes in various eukaryotic organisms. Despite of its significance, current understanding of the biological functions and regulatory mechanisms of the CSN complex is still very limited. To unravel these molecular mechanisms, we have performed a comprehensive proteomic analysis of the human CSN complex using a new purification method and quantitative mass spectrometry. Purification of the human CSN complex from a stable 293 cell line expressing N-terminal HBTH-tagged CSN5 subunit was achieved by high-affinity streptavidin binding with TEV cleavage elution. Mass spectrometric analysis of the purified CSN complex has revealed the identity of its composition as well as N-terminal modification and phosphorylation of the CSN subunits. N-terminal modifications were determined for seven subunits, six of which have not been reported previously, and six novel phosphorylation sites were also identified. Additionally, we have applied the newly developed MAP-SILAC and PAM-SILAC methods to decipher the dynamics of the human CSN interacting proteins. A total of 52 putative human CSN interacting proteins were identified, most of which are reported for the first time. In comparison to PAM-SILAC results, 20 proteins were classified as stable interactors, whereas 20 proteins were identified as dynamic ones. This work presents the first comprehensive characterization of the human CSN complex by mass spectrometry-based proteomic approach, providing valuable information for further understanding of CSN complex structure and biological functions.

*Correspondence should be addressed to Dr. Lan Huang (e-mail: E-mail: lanhuang@uci.edu) Medical Science I, D233, Department of Physiology & Biophysics, Department of Developmental & Cell Biology, University of California, Irvine, Irvine, CA 92697-4560. Phone: 949-824-8548. Fax: 949-824-8540.
[†]Departments of Physiology & Biophysics and Developmental & Cell Biology, University of California.
[‡]Mount Sinai School of Medicine.
[§]Department of Biological Chemistry, University of California.

Supporting Information Available: Supplemental Figure 1. Identification of three N-terminal peptides of subunit CSN5. MS/MS spectra of (A) N-terminal peptide of tagged CSN5 (MH_3^{3+} 782.37 GSHHHHHHLINMAASGSGMAQK); (B) N-terminus of endogenous CSN5 with N-acetylation (MH_2^{2+} 475.23 Acetyl-AASGSGMAQK); (C) Free N-terminus of endogenous CSN5 (MH_2^{2+} 519.74 MAASGSGMAQK). Supplemental Figure 2, MS/MS spectra of the identified N-terminal peptides. Supplemental Figure 3, MS/MS spectra of the identified phosphopeptides. Supplemental Figure 4, validation of the dynamic interaction of Cul-4A with the CSN complex. Comparison of incorporation of myc-Cul-4A expressed in the control cells into the HBTH-CSN5 containing complexes during the purification using the Tc-PAM approach at three different incubation times (20 min, 1 h, and 2 h) and the MAP approach (2 h). The top blot was probed with myc-HRP antibody to detect Myc-tagged Cul-4A, whereas the bottom one was probed with anti-RGSHis to detect the tagged CSN5 for sample loading control. Supplemental Figure 5, validation of the selected CSN interacting proteins. The purified protein complexes from 293^{HTBH} cells (lane 1) and $293^{HBTB\text{-}CSN5}$ cells (lane 2) were subjected to 1-D SDS-PAGE and Western blot. The blots were probed with anti-DAPK1 (top one), and anti- DOCK7 (bottom one), respectively. Supplemental Table 1, protein reports of the identified CSN interacting proteins using MAP-SILAC and PAM-SILAC approaches. Supplemental Table 2, quantifying putative CSN interacting proteins using MAP-SILAC and PAM-SILAC approaches. This material is available free of charge via the Internet at http://pubs.acs.org.

Keywords

COP9 Signalosome; cullin-containing ubiquitin ligase; MAP-SILAC; PAM-SILAC; affinity purification; phosphorylation; quantitative mass spectrometry; dynamic interaction; CSN interacting proteins

Introduction

The COP9 signalosome (CSN), previously known as the COP9 complex or JAB1-containing signalosome, is an evolutionally conserved protein complex that exists in all eukaryotes.[1] The CSN complex localizes mainly in and close to the nucleus, whereas some subunits have been found to be cytosolic. With a molecular weight of ~450 kDa, the CSN consists of eight subunits (CSN1–8). In mammals, the CSN7 subunit is encoded by two similar genes, CSN7a and CSN7b. Although it was originally discovered in *Arabidopsis* as a repressor required for the repression of photomorphogenic seedling development in the dark, the CSN complex has now been recognized as an essential protein complex involved in diverse cellular and developmental processes in various eukaryotic organisms, including early development, DNA repair, cytokine signaling, regulation of nuclear transport, cell cycle progression, angiogenesis, cellular homeostasis and antigen-induced responses.[1–3] Deletions of CSN subunits cause drastic alternations in the gene expression profile and early lethality of multicellular model organisms such as *Arabidopsis*, *Drosophila*, and mouse. Recent evidence has suggested that the CSN plays a significant role in the regulation of various cancers and might be an attractive therapeutic target for cancer treatment.

The CSN complex has been found to be structurally related to two multisubunit protein complexes, the 19S proteasome regulatory complex and the eukaryotic translation initiation factor 3 (eIF3).[1,4] The 19S proteasome regulatory complex assembles with the 20S catalytic core to form the 26S proteasome, a multicatalytic proteinase responsible for the degradation of ubiquitinated substrates.[5] The eIF3 complex is involved in both ribosome biogenesis and protein synthesis in eukaryotes, and functions as a docking site for assembling other eIFs during translation initiation.[6] Sequence homology analysis[4] has revealed that the CSN is evolutionarily closer to the proteasome lid, the subcomplex of the 19S regulatory complex positioned at the exterior ends of the 26S proteasome. They share a common architecture containing six subunits that harbor PCI (proteasome, COP9 signalosome, initiation factor 3) domain at their C-terminus and two subunits containing MPN (Mpr1-Pad1-N-terminal) domains.[4] In addition, each of the eight CSN subunits shares pairwise sequence homology with a corresponding lid component. Interestingly, only some of the eIF3 subunits contain the two signature domains with three PCI and two MPN proteins, different from the stoichiometry [6 (PCI) +2 (MPN)] in the CSN and the proteasome lid complexes. It has been shown that the PCI domain is important for the assembly of the CSN complex, whereas the MPN domain with a catalytic JAMM/MPN$^+$ motif in subunit CSN5 is responsible for metalloprotease activity.[1,7–9] Despite common homology domains and similar structures, the functions of the three complexes are significantly different. Interactions of the proteasome and eIF3 with the CSN have been noted.[10,11] However, the biological significance of such interactions remains to be elucidated.

The CSN complex has been well-characterized as the deneddylase responsible for removing Nedd8 covalently attached to cullin family proteins, thus regulating the activities of cullin-based ubiquitin E3 ligases.[12,13] It therefore controls substrate specificity and stability in the ubiquitin-proteasome dependent degradation pathway. This function has been proposed to be mediated by the catalytic subunit CSN5 but requires the assembly of the entire CSN holocomplex.[1,9] In addition to the deneddylase activity, other functions have been reported to

be associated with the CSN including kinase and deubiquitinating activities.[14–16] The CSN associates with kinases that can phosphorylate p53, c-Jun and other regulatory proteins,[14] and interacts with deubiquitinating enzymes that can cleave linear and branched ubiquitin chains.[15,16]

Since its first discovery in plants, CSN has gained substantial attention due to its multiple functions in diverse cellular processes. However, the molecular details in its biochemical functions and regulatory mechanisms are largely unknown. Proteomic characterization of the human CSN complex will be essential for establishing molecular basis to understand its functional diversity. Surprisingly, such studies are currently lacking. Here we report a comprehensive proteomic analysis of the human CSN complex using affinity purification and tandem mass spectrometry to characterize subunit composition and posttranslational modifications. In addition, newly developed SILAC-based strategies have been employed to investigate the human CSN interacting proteins.

Experimental Procedures

Chemicals and Reagents

ImmunoPure streptavidin, HRP conjugated antibody and Super Signal West Pico chemiluminescent substrate were purchased from Pierce Biotechnology (Rockford, IL). Sequencing grade trypsin was purchased from Promega Corp. (Madison, WI). Endoproteinase Lys-C was from WAKO chemicals (Osaka, Japan). $^{13}C_6{}^{15}N_4$-arginine and $^{13}C_6{}^{15}N_2$-lysine were purchased from Cambridge Isotope Laboratories (Andover, MA). $^{12}C_6{}^{14}N_4$-arginine and $^{12}C_6{}^{14}N_2$-lysine were from Sigma (St. Louis, MO). Myc-HRP antibody was generously provided by Dr. Haoping Liu at UC Irvine, and anti-DOCK7 antibody was a generous gift from Dr. Linda Van Aelst at Cold Spring Harbor Laboratory. Anti-RGSHis and anti-DAPK1 antibodies were purchased from Qiagen (Valencia, CA) and Sigma, respectively. All other general chemicals for buffers and culture media were from Fisher Scientific or VWR International.

Plasmid and Cloning

Human CSN5 was PCR amplified using a GeneStorm clone (GeneStorm accession: U65928) as the template with the following primers: forward, 5′-TATA TTAATTAA C ATG GCGGCGTCCGGGAGC-3′; and reverse, 5′-GTCA GATATC TTAAGAGATGTTAATTTG-3′ A CSN5 DNA fragment containing a Pac I site at the 5′ end and an EcoR V site at the 3′ end was cloned into HBTH-pQCXIP, a derivative of pQCXIP (Clontech, Mountain View, CA).[17] A schematic representation of HBTH-CSN5 is shown in Figure 1A.

Generation of Retrovirus for Protein Expression and 293 Stable Cell Lines

The procedure for making the retrovirus and generating 293 stable cell lines has been reported previously.[17] Briefly, a 293 GP2 cell line was cotransfected with pQCXIP-HBTH-CSN5 and a plasmid expressing VSV-G. The retrovirus was produced and released to the medium between 36 to 96 h after transfection. The medium containing the retrovirus was then used to transduce 293 cells, which were subsequently selected with puromycin to establish the stable cell line expressing HBTH-CSN5 ($293^{HBTH\text{-}CSN5}$). The stable 293 cell line stably expressing HTBH (293^{HTBH}) was also generated.

Tandem Affinity Purification of the Human CSN Complex

The $293^{HBTH\text{-}CSN5}$ and 293^{HTBH} cells were grown to confluence in DMEM medium containing 10% FBS and 1% penicillin/streptomycin, then trypsinized and washed three times

with PBS buffer. The cell pellets were collected and lysed in lysis buffer (100 mM NaCl, 25 mM Tris-HCl, 10% glycerol, 5 mM ATP, 1 mM DTT, 5 mM $MgCl_2$, 1× protease inhibiter (Roche), 1× phosphatase inhibitor, 0.35% NP-40, pH 8.0). The lysates were centrifuged at 13 000 rpm for 15 min to remove cell debris and the supernatant was incubated with streptavidin resins for 2 h (optimal incubation time) at 4 °C. The streptavidin resins were then washed with 50 bed volumes of the lysis buffer, followed by a final wash with 30 bed volumes of TEB buffer (50 mM Tris-HCl, pH 8.0) containing 10% glycerol. The protein bound resin was incubated in 2 bed volumes of TEB buffer with 1% TEV at 30 °C for 1 h. The CSN complex was eluted from the beads with TEB buffer and stored in 10% glycerol at −80 °C.

Cell Culture and Metabolic Stable Isotope Labeling Using SILAC

The $293^{HBTH\text{-}CSN5}$ cells were grown in DMEM supplemented with 28 μg/mL $^{12}C_6{}^{14}N_4$-arginine, 73 μg/mL $^{12}C_6{}^{14}N_2$-lysine, 10% dialyzed fetal bovine serum, and 1% penicillin/streptomycin (light medium). The 293^{HTBH} cells were grown in DMEM supplemented with 28 μg/mL $^{13}C_6{}^{15}N_4$-arginine, 73 μg/mL $^{13}C_6{}^{15}N_2$-lysine, 10% dialyzed fetal bovine serum, and 1% penicillin/streptomycin (heavy medium). Cell lines were grown for more than seven doublings in the labeling media to ensure complete labeling. The cells were then treated the same way as described above for protein purification.

PAM (Purification after Mixing)-SILAC and MAP (Mixing after Purification)-SILAC Experiments

For PAM-SILAC experiments, equal amounts of cell lysates from $293^{HBTH\text{-}CSN5}$ and 293^{HTBH} cells were mixed, and followed by affinity purification as described above. For MAP-SILAC experiments, purification of each sample from equal amount of cell lysates was carried out separately before the purified samples were mixed for subsequent digestion and mass spectrometric analysis. The same cell lysates from each type of cells were equally divided for PAM-SILAC and MAP-SILAC experiments. More details can be found in a previous publication.[18] Twenty 150-mm plates of $293^{HBTH\text{-}CSN5}$ or 293^{HTBH} cells were used for a set of MAP-SILAC and PAM-SILAC experiments, which have been reproduced three times.

Liquid Chromatography and Tandem Mass Spectrometry (LC-MS/MS)

The purified human CSN complex was further separated by 1-D SDS-PAGE (12%) and the protein bands were visualized by Coomassie Brilliant Blue staining. The procedures for in-gel trypsin digestion and in-solution Lys-C/trypsin digestion have been described previously.[17] The in-solution peptide digests were first separated by strong cation exchange (SCX) chromatography with a 2.1 mm × 10 cm polysulfethyl A column (Nest Group) at a flow rate of 200 μL/min using AKTA Basic 10 (GE Healthcare). Peptide elution was achieved by a salt gradient and 15 fractions were manually collected based on UV absorbance at 215 nm. All of the SCX fractions were subsequently desalted using Vivapure C_{18} microspin columns (Vivascience) prior to MS analysis. Initial LC MS/MS analysis was performed using nanoflow reverse phase liquid chromatography (RPLC) (Dionex, CA) coupled online with QSTAR XL (PE Sciex/Applied Biosystems) using a capillary column (75 μm i.d. × 150 mm length) packed with C18 resins (GL Sciences). The peptides were eluted using a linear gradient of 0% to 35% B in 80 min at a flow rate of 250 nL/min (solvent A, 98% H_2O/2% acetonitrile/0.1% formic acid; solvent B, 98% acetonitrile/2% H_2O/0.1% formic acid). The MS/MS was operated in an information-dependent mode in which each full MS analysis was followed by three MS/MS acquisitions where the three most abundant peptide molecular ions were dynamically selected for collision induced dissociation (CID) to generate tandem mass spectra. The SILAC samples were analyzed by LC-MS/MS using a nanoLC system (Eksigent, Inc.) coupled with Linear Ion Trap (LTQ)-Orbitrap XL mass spectrometer (Thermo-Electron Corp). The LC analysis was performed using a capillary column (100 μm i.d. × 150 mm length) packed with C18 resins

(GL Sciences) and the peptides were eluted using a linear gradient of 2–35% B in 105 min; (solvent A, 100% H_2O/0.1% formic acid; solvent B, 100% acetonitrile/0.1% formic acid). A cycle of one full FT scan mass spectrum (350–2000 *m*/*z*, resolution of 60 000 at *m*/*z* 400) was followed by 10 data-dependent MS/MS acquired in the linear ion trap with normalized collision energy (setting of 35%). Target ions selected for MS/MS were dynamically excluded for 30 s.

Database Searching for Protein Identification and Quantification

Monoisotopic masses of parent ions and corresponding fragment ions, parent ion charge states and ion intensities from LC-MS/MS spectra were extracted using in-house software based on Raw_Extract script from Xcalibur v2.4. QSTAR MS/MS data was extracted and analyzed as described.[18] Following automated data extraction, the resultant peak lists for each LC-MS/MS experiment were submitted to the development version (5.0.0) of Protein Prospector (UCSF) for database searching using a Swiss-Prot database (11/07/2007, 574 100 sequence entries). *Homo sapiens* was selected as the restricted species. Trypsin was set as the enzyme with a maximum of two missed cleavage sites. The mass tolerances for parent and fragment ions were set at ±100 ppm/±300 ppm for QSTAR data, and ±20 ppm/±0.8 Da for LTQ-Orbitrap data. Chemical modifications such as protein N-terminal acetylation, methionine oxidation, N-terminal pyroglutamine, and deamidation of asparagine were selected as variable modifications. For SILAC experiments, $^{13}C_6{}^{15}N_4$-labeled Arg and $^{13}C_6{}^{15}N_2$-labeled Lys were also chosen as variable modifications. No fixed modifications were selected. The Search Compare program in Protein Prospector was used for summarization, validation and comparison of results. To determine the expectation value cutoff that corresponds to a percent false positive (% FP) rate, each project was searched against a normal database concatenated with the reversed form of the database. An algorithm in Search Compare automatically plots the expectation values versus % FP rate for each search result. On the basis of these results, we chose an expectation value cutoff corresponding to ≤0.2% FP for all peptides. At this false positive rate, false protein hits from the decoy database were not observed. General protein identification was based on at least two peptides. If a protein is identified by multiple peptides from more than two preparations, it would be considered as a hit in a preparation identified by only one peptide. Homologous proteins were reported using the same rules as described.[19] For SILAC experiments, the Search Compare program was also used to calculate the relative abundance ratios of Arg/Lys-containing peptides based on ion intensities of monoisotopic peaks observed in the LC MS spectra. The peptide peak intensities were averaged across the selected elution profile (20 s).[20] Signal-to-noise ratio ≥5 was required for peaks to be considered for quantitation. The Search Compare program also corrects for the isotopic purity of the heavy SILAC amino acids, which was set to 98% purity. The SILAC ratios were further validated by checking all of the raw spectra within the Search Compare program. The ratio outliers (with >30% standard deviations) could be easily visualized on the ratio plots in Protein Prospector and then excluded for further calculation. If the peptide peaks were mixed with other peptide peaks or buried in the noise peaks, they were excluded for quantification. The SILAC ratios reported here were average values, and the accuracy and significance of the measurements were evaluated using standard deviations. The ratios obtained from replicate experiments were examined manually. The resulting SILAC ratios were further corrected by differences in protein concentrations between two cell lysates for comparison.

Transfection of Myc-Cul-4A for Quantitative Western Blotting

The 293^{HTBH} cells were transiently transfected with pcDNA-myc-Cul-4A. Twenty-four hours after transfection, the cells were washed three times in PBS and lysed in buffer A as described above. The lysates were centrifuged at 13 000 rpm for 15 min to remove cell debris. Cleared lysate was divided into four aliquots (lysate A). Equal amount of lysates from $293^{HBTH\text{-}CSN5}$ was processed similarly (lysate B). In Tc-PAM experiments, equal amounts of lysates A and B were combined and incubated with streptavidin resins for 20 min, 1 h, and 2

h at 4 °C, respectively. In MAP experiments, equal amounts of lysates A and B were subjected to purification separately by incubating with streptavidin resins for 2 h.

Validation of Dynamic Proteins Using Quantitative Western Blotting

The purified samples were separated by 1-D SDS-PAGE. Proteins were then transferred to a PVDF membrane and analyzed by immunoblotting. Myc-Cul-4A protein was detected using a myc-HRP antibody (1:4000). The blots were then stripped and reprobed with anti-RGSHis (1:1000) followed by HRP-conjugated antimouse IgG (1: 10 000) to detect the tagged CSN5 for sample loading control.

Validation of CSN Interacting Proteins

Two novel CSN complex interacting proteins, DAPK1 and DOCK7, were selected for validation by immunoblotting. The purified CSN5 complex was subjected to Western blot and probed with specific antibodies against DAPK1 and DOCK7, respectively.

Results

1. Purification and Identification of the Human CSN Complex

In this work, a derivative of the HB tag,[21,22] that is, HBTH, was generated to tag the CSN5 subunit at its N-terminus for affinity purification (Figure 1A). The N-terminal HBTH tag consists of two hexahistidine tags, a TEV cleavage site, and a signal sequence for *in vivo* biotinylation, similar to the C-terminal HTBH tag developed for purification of human proteasome complexes.[17] To minimize overexpression of HBTH-CSN5, a 293 stable cell line expressing HBTH-CSN5 ($293^{\text{HBTH-CSN5}}$) was produced using retrovirus infection. It should be noted that subunit CSN5 has not been previously used as bait for the purification of the CSN complex. Because of CSN5's functional significance, its use as the purification bait would be advantageous for capturing specific interacting proteins that may regulate the CSN function. Similar to the proteasome complexes,[17] affinity purification of the human CSN complex was also achieved with a single-step purification by binding to streptavidin resins and TEV cleavage elution under native condition as shown in Figure 1B. The overall 1D gel pattern of the purified CSN complex was very similar to that previously reported.[23–26]

A comprehensive mass spectrometric analysis of the purified CSN complexes was carried out to characterize subunit composition and post-translational modifications using 2-D LC-MS/MS. The results are summarized in Table 1. As shown, a complete subunit composition of the CSN complex has been captured. The results corresponded well with the proteins identified by in-gel digestion/mass spectrometry (Figure 1B).

2. Identification of the N-Terminal Peptides of the CSN Subunits

N-terminal post-translational modification is commonly observed in eukaryotic proteins.[27] However, characterization of such modifications in human CSN subunits is lacking. In this study, nine N-terminal peptides have been identified, seven of which have not been previously reported. As an example, Figure 2A displays the ESI MS/MS spectrum of a tryptic peptide with MH_2^{2+} 681.85. The sequence was unambiguously determined as Acetyl-ASALEQFVNSVR, matched to the N-terminus of subunit CSN3, where it is acetylated after removal of the first methione residue. Similarly, subunit CSN7a is N-acetylated, whereas subunit CSN1 and CSN8 have a free N-terminus after the removal of the first methionine residue.

In contrast to only one N-terminus for one subunit, two different N-termini were identified for subunit CSN7b in the purified complexes. The MS/MS spectra of the two corresponding peptides (MH_2^{2+} 1043.58 and MH_2^{2+} 1064.58) were shown in Figure 2B,C. The overall

fragmentation patterns of the two peptides are very similar, with identical y ions, whereas the b ions show a 42 Da shift, suggesting that the difference between these two peptides is at the N-terminus. The peptide sequences were determined as AGEQKPSSNLLEQFILLAK and Acetyl-AGEQKPSSNLLEQFILLAK, matched to the N-terminus of subunit CSN7b. The different CSN7b N-termini have been reproducibly observed in multiple purifications, indicating that isoforms of CSN7b exist in the purified CSN complexes. In comparison to the free N-terminal peptide, the N-acetylated form of CSN7b seems to be much more abundant since it has been detected in all preparations with higher ion intensities in the MS analyses.

Three different N-terminal peptides were captured and identified for subunit CSN5 (Supplemental Figure 1 in Supporting Information). One of them is generated from the tagged CSN5, whereas the other two were from the endogenous CSN5 containing different N-termini, one with the removal of methionine and N-acetylation, and the other with methionine remaining but no acetylation. In comparison to the N-acetylated form, the unprocessed N-terminal peptide appears to be much more dominant. Since CSN5 was tagged at its N-terminus for the purification in our study, the discovery of three N-terminal forms of CSN5, that is, tagged, N-acetylated, and free forms, implies that some of the tagged CSN5 may be present as an oligomer with the endogenous CSN5 by itself or the CSN complex may be a dimer. The identified N-terminal peptides are summarized in Table 2 and Supplemental Figure 2.

3. Identification of Phosphorylation Sites of the CSN Subunits

Because of the associated kinases, it is thought that the CSN has kinase activities.[28,29] It has also been suggested that CSN subunits can be phosphorylated.[29] Despite of its importance in signal transduction, no detailed analysis has been carried out so far to determine phosphorylation of the CSN complex. In this work, phosphorylation of CSN subunits was characterized by direct MS analysis of peptide digests of the purified CSN complex. Figure 3A illustrates the MS/MS spectrum of a tryptic peptide (MH_2^{2+} 820.85) from the CSN peptide digest. A fragment ion labeled as [MH_2^{2+}]* (i.e., MH_2^{2+} 772.03) was obtained due to the loss of H_3PO_4 (−98 Da) from the parent ion (MH_2^{2+} 820.85), indicating that the peptide is phosphorylated. On the basis of the series of b and y ions, the peptide was determined as the phosphorylated form of the peptide ^{452}EGSQGELTPANSQSR^{466}, matched to the sequence of subunit CSN1. There are four potential phosphorylation sites in this sequence. From the nonphosphorylated forms of b_4~b_7 and y_2~y_5, y_7 ions, the phosphorylation most likely occurs on Thr459. The detection of phosphorylated forms of b_8~b_{11}, y_8~y_{11}, y_{13} and their neutral loss ions confirms this assignment unambiguously. Phosphorylation on Thr459 is consistent with the results from a global phosphoproteome analysis.[30] Our analysis has also determined a novel phosphorylation site of subunit CSN3 (Figure 3B). The sequence was identified as ^{407}SMGSQEDDSGNKPSSYpS^{423}, where the C-terminal Ser423 is phosphorylated. A total of seven unique phosphorylation sites have been identified as summarized in Table 3, and six of them are novel. The corresponding MS/MS spectra of the identified phosphorylated peptides are shown in Supplemental Figure 3 in Supporting Information.

4. Quantitative Identification of Specific Interacting Proteins of the CSN Complex Using MAP-SILAC and PAM-SILAC Approaches

Protein–protein interaction has been recognized as one of the key regulatory mechanisms for modulating protein functions. It is evident that CSN interacting proteins directly affect its biochemical activities.[15,16,28,29] However, current knowledge of CSN interacting proteins is mostly limited to the results obtained from *in vitro*, two-hybrid and immunoblotting experiments. Affinity purification and SILAC-based quantitative mass spectrometry was employed in this work to identify CSN complex interacting proteins since this strategy is powerful for identifying specific protein interactions.[18,19,22] To determine the nature of protein interactions, MAP-SILAC and PAM-SILAC experiments were carried out (Figure 4).

It has been shown that dynamic interacting proteins can exchange between the light and heavy forms during purification when both are present in PAM-SILAC experiments, thus leading to low PAM-SILAC ratios.[18] However, such an interaction exchange is prevented in MAP-SILAC approach, which permits the preservation of specificity of protein interactions during purification and allows for easy identification based on their SILAC ratios, regardless of the nature of their interactions. Therefore, specific stable interactors do not change their SILAC ratios between MAP-SILAC and PAM-SILAC experiments; while specific but dynamic protein interactions have MAP-SILAC ratios significantly higher than their PAM-SILAC ratios. These characteristic differences allow one to effectively distinguish stable and dynamic interactors.[18]

Figure 5A1–2 displays the MS spectra of a selected peptide matched to subunit CSN2. Its MAP-SILAC and PAM-SILAC ratios are high, meaning that CSN2 was selectively enriched from the $293^{HBTH\text{-}CSN5}$ cells. Similarly, all of the CSN subunits have high SILAC ratios in both experiments and are classified as stable subunits (Type I), suggesting that the CSN complex is a stable entity. In addition, a total of 52 proteins with MAP-SILAC ratios >1.5 have been identified as putative CSN interacting proteins (Table 4 and Supplemental Table 2 in Supporting Information), 44 of which have not been previously reported. Twenty proteins have comparable MAP-SILAC and PAM-SILAC ratios and thus have been classified as stable interacting partners (Type II) (an example is given in Figure 5B1–2). A group of proteins bound to affinity matrix nonspecifically are classified as background proteins (Type III), whose SILAC ratios were ≤1.5 in MAP and PAM experiments (Figure 5C1–2). In addition, type IV proteins have MAP-SILAC ratios significantly higher than their PAM-SILAC ratios (>2 -fold) (Table 4). As an example shown in Figure 5D1–2, the MAP-SILAC ratio of Cul-4A was high, whereas its PAM-SILAC ratio was 1.8. The significant difference in MAP-SILAC and PAM-SILAC ratios indicates that Cul-4A is a dynamic interactor of the CSN5 containing complexes.

5. Validation of the Dynamic CSN Interacting Proteins

One of the identified dynamic interactors, Cul-4A, has been selected for further validation using transfection and immunoblotting.[18] In the validation experiments, the control 293^{HTBH} cells were transfected with myc-Cul-4A, while the $293^{HBTH\text{-}CSN5}$ cells did not contain any tagged Cul-4A. Cell lysates from the 293^{HTBH} and $293^{HBTH\text{-}CSN5}$ cells were analyzed by either Time-controlled (Tc)-PAM or MAP experiments. The final purified samples from both Tc-PAM and MAP experiments were then subjected to gel electrophoresis and immunoblotting using specific antibodies against myc tag to determine the interaction swapping of the tagged Cul-4A with their endogenous counterparts during purification. Because the CSN complexes were selectively purified from cells expressing no myc-tagged proteins, any copurification of myc-Cul-4A must be a result of interactions formed in the mixed lysates during the incubation. Supplemental Figure 4 in Supporting Information shows the myc-HRP Western blot that demonstrates the incorporation of myc-Cul-4A into the purified CSN complex occurs only in PAM but not in MAP experiments. These results unambiguously validated the dynamic interaction of Cul-4A with the CSN complex. Similar results were obtained using HA tagged Cul-1 (data not shown), suggesting that the dynamic interaction with CSN complex may be a general feature for cullins.

6. Validation of Newly Identified CSN Interacting Proteins

Two novel CSN complex interacting proteins, DAPK1 and DOCK7, have been selected for further validation. DAPK1 is a calcium/calmodulin-dependent serine/threonine kinase which acts as a positive regulator of apoptosis;[31] and DOCK7 is a Rac GTPase activator involved in regulating axon formation [32]. The purified CSN5 containing CSN complexes were subjected to 1D SDS-PAGE and analyzed by immunoblotting using anti-DAPK1 or anti-DOCK7 antibodies. Copurification of DAPK1 and DOCK 7 with the CSN complexes was confirmed

in comparison to results from tag-alone controls (Supplemental Figure 5 in Supporting Information).

Discussion

By using a newly developed affinity purification strategy,[17] isolation of the human CSN complex was achieved with the N-terminal HBTH tagged CSN5 stably expressed in 293 cells. In contrast to conventional and antibody-based immunoaffinity methods,[24,25] our purification approach is fast and effective, and requires less starting material. In comparison to the purification using FLAG-tagged subunits,[10,24,26] the HB tag is versatile for the isolation of protein complexes and can be used under both native and denatured conditions.[17,22]

In this work, nine CSN subunits (i.e., CSN1, CSN2, CSN3, CSN4, CSN5, CSN6, CSN7a, CSN7b, and CSN8) have been captured and identified using HTBH-CSN5. Aside from the CSN composition, N-terminal processing of the CSN subunits was investigated. The N-terminal modifications of six subunits (CSN1, CSN4, CSN5, CSN7a, CSN7b, and CSN8) were identified for the first time for mammalian CSN components. Two of the CSN subunits, CSN7b and CSN5, appear to have two different N-terminal processed forms, either acetylated or free at N-terminus. This novel finding suggests the presence of a heterogeneous population of CSN complexes due to different N-terminal processing. Interestingly, similar results have been obtained for human proteasome subunits,[17,33] implying that dual N-terminal processing of a protein may be a general phenomenon for mammalian proteins. Apart from the large CSN holocomplex, small complexes containing a subset of CSN subunits have been found in various species including mammalian cells.[1,34] We suspect that the subunit isoforms due to N-terminal processing may be incorporated into subpopulation of the CSN complexes and the heterogeneity of the CSN complex appears to be much more complicated than expected.

Phosphorylation of CSN subunits has also been investigated. A total of six novel phosphorylation sites from three subunits (i.e., CSN1, CSN3, and CSN8) have been determined. These results provide the first direct evidence of *in vivo* phosphorylation of CSN subunits in the context of the CSN complex. As shown in Table 2, 10 phosphopeptides have been identified in subunit CSN1, representing four unique phosphorylation sites. Kinase consensus sequence analysis has revealed that the identified phosphorylated residues in CSN1 are serine or threonine residues followed either by proline, indicative of phosphorylation by mitogen-activated or cyclin dependent kinases (MAP kinases and CDKs), or by glutamine, the consensus sites for DNA-PK or ATM. Given the key role MAP kinases and CDKs have in cell proliferation and the importance of DNA-PK and ATM in DNA damage response, it is tempting to speculate that CSN1 phosphorylation might be subjected to cell cycle and/or DNA damage dependent regulation. CSN1 has an essential role in the CSN complex assembly;[35,36] therefore, the phosphorylation of CSN1 may lead to conformational changes in the complex to fulfill different functions at various physiological states.

To comprehend the underlying mechanisms of CSN functions, we have profiled the CSN interacting proteins, including both dynamic and stable ones using MAP-SILAC and PAM-SILAC.[18] Fifty-two proteins have been identified as putative CSN interacting proteins including components of cullin-based E3 ligases, and proteins involved in various biological processes such as apoptosis, signal transduction, DNA replication and repair, and cell differentiation. This is the first report on human CSN interacting proteins using affinity purification and quantitative mass spectrometry. On the basis of the characteristic ratio changes, 20 proteins were grouped as dynamic proteins. Among them are five of the eight cullin family members, that is, Cul-1, Cul-2, Cul-3, Cul-4A, and Cul-4B. Cullins are the key components of cullin-based E3 ubiquitin ligases that are responsible for substrate specificity of the ubiquitin-proteasome dependent degradation pathway.[9] They are believed to interact

with the CSN complex during the deneddylation process. Identification of five cullins from the purified CSN complexes offers direct evidence of their interactions. The absence of Cul-5, Cul-7 and Parc in the purified samples is most likely due to their low abundance.[37] All of the cullin proteins identified here share the same feature of dynamic interactions with the human CSN complex. In addition, several components of cullin-based E3 ligases such as DDB1, DDB2, Rbx1 and F-box only protein 46 have also been found to interact dynamically with the CSN in a similar manner as the cullins. This is not surprising since these proteins assemble with cullins to form E3 ubiquitin ligases as a functional entity. The assembly and disassembly of cullin-based E3 ligases is a dynamic process that is partially controlled by cycles of neddylation and deneddylation.[9,38] We suspect that the dynamic characteristics of the cullins' interaction with the CSN may be required for fine regulation of its biological activities during the cycle of activation and inactivation of cullin-containing E3 ligases. Interestingly, protein VPRBP, also called DDB1 and Cul-4 associated factor 1, has been determined as a stable interactor of the CSN, indicating that it does not interact with the CSN in a similar manner as the other cullin E3 ligase components. Protein VPRBP has been suggested as a receptor for Cul4-DDB1 ubiquitin ligase complex;[39] therefore, it likely functions as an adaptor protein to facilitate the interaction between the CSN and Cul-4.

Another dynamic interactor is cell death-associated protein kinase1 (DAPK1), the identification of which in the purified CSN complexes has been confirmed by Western blotting. DAPK1 appears to have multiple functions in cell survival, tumor suppression, cell motility, and cytoskeletal organization and its activity can be regulated by cellular calcium levels, autophosphorylation, ubiquitination, and proteasomal degradation.[40] In addition, DAPK1 has been implicated in regulating apoptosis induced by a variety of stimuli. Recently, subunit CSN6 has been reported to be cleaved by activated caspases during apoptosis.[2] The processing of CSN6 precedes the caspase-dependent cleavage of Rbx1 and results in the stimulation of the deneddylation activity. Therefore, the interaction of DAPK1 and CSN may play a role in regulating CSN activity during apoptosis.

In summary, we have developed an effective method to rapidly isolate the human CSN complex under native condition from a stable cell line expressing a HB tagged CSN subunit. This approach enables us to effectively carry out a comprehensive analysis of the purified complexes for elucidating CSN subunit composition, post-translational modifications as well as identification of putative CSN interacting proteins. We show the capability of identifying and distinguishing CSN dynamic and stable interactors using MAP-SILAC and PAM-SILAC approaches. The quantitative classification offers a unique angle to probe and understand CSN interacting proteins. The new and detailed proteomic information of the human CSN complex is of significant importance to the design of future experiments for further elucidation of assembly and regulation mechanisms of the human CSN complex under various physiological conditions.

Supplementary Material

Refer to Web version on PubMed Central for supplementary material.

Acknowledgements

We thank the Huang laboratory members for their help during this study. We thank Prof. A. L. Burlingame, Peter Baker and Aenoch Lynn for the development version of Protein Prospector, Dr. Shenheng Guan for the script to extract orbitrap LC-MS/MS data. We are very grateful to Prof. Steve Gygi and Dr. Judit Villen for their help in optimizing LTQ-Orbitrap performance. This work is supported by National Institutes of Health grants (GM-74830 and S10RR023552 to L.H.) and Dept. of the Army (PC-041126 to L.H.).

Abbreviations

CSN
signalosome

293$^{HBTH-CSN5}$
293 cells stably expressing HBTH-CSN5

293^{HTBH}
293 cells stably expressing HTBH

PCI
Proteasome-COP9 signalosome-Initiation factor 3

MPN
Mpr1-Pad1-N-terminal

HB
histidine and biotin tag

LC-MS/MS
liquid chromatography-tandem mass spectrometry

HRP
horseradish peroxidase

SCX
strong cation exchange

m/z
mass/charge

TEV
tobacco etch virus

TEB
TEV elution buffer

SILAC
stable isotope labeling of amino acids in cell culture

MAP
mixing after purification

PAM
purification after mixing

Tc-PAM
time controlled-purification after mixing

References

1. Wei N, Deng XW. The COP9 signalosome. Annu Rev Cell Dev Biol 2003;19:261–86. [PubMed: 14570571]
2. Hetfeld BK, Peth A, Sun XM, Henklein P, Cohen GM, Dubiel W. The COP9 signalosome-mediated deneddylation is stimulated by caspases during apoptosis. Apoptosis 2008;13(2):187–95. [PubMed: 18060501]

3. Richardson KS, Zundel W. The emerging role of the COP9 signalosome in cancer. Mol Cancer Res 2005;3(12):645–53. [PubMed: 16380502]
4. Scheel H, Hofmann K. Prediction of a common structural scaffold for proteasome lid, COP9-signalosome and eIF3 complexes. BMC Bioinf 2005;6:71.
5. Pickart CM, Cohen RE. Proteasomes and their kin: proteases in the machine age. Nat Rev Mol Cell Biol 2004;5(3):177–87. [PubMed: 14990998]
6. Valasek L, Hasek J, Nielsen KH, Hinnebusch AG. Dual function of eIF3j/Hcr1p in processing 20 S pre-rRNA and translation initiation. J Biol Chem 2001;276(46):43351–60. [PubMed: 11560931]
7. Cope GA, Deshaies RJ. COP9 signalosome: a multifunctional regulator of SCF and other cullin-based ubiquitin ligases. Cell 2003;114(6):663–71. [PubMed: 14505567]
8. Lyapina S, Cope G, Shevchenko A, Serino G, Tsuge T, Zhou C, Wolf DA, Wei N, Shevchenko A, Deshaies RJ. Promotion of NEDD-CUL1 conjugate cleavage by COP9 signalosome. Science 2001;292 (5520):1382–5. [PubMed: 11337588]
9. Petroski MD, Deshaies RJ. Function and regulation of cullin-RING ubiquitin ligases. Nat Rev Mol Cell Biol 2005;6(1):9–20. [PubMed: 15688063]
10. Huang X, Hetfeld BK, Seifert U, Kahne T, Kloetzel PM, Naumann M, Bech-Otschir D, Dubiel W. Consequences of COP9 signalosome and 26S proteasome interaction. FEBS J 2005;272(15):3909–17. [PubMed: 16045761]
11. Yahalom A, Kim TH, Roy B, Singer R, von Arnim AG, Chamovitz DA. Arabidopsis eIF3e is regulated by the COP9 signalosome and has an impact on development and protein translation. Plant J 2008;53 (2):300–11. [PubMed: 18067529]
12. Pan ZQ, Kentsis A, Dias DC, Yamoah K, Wu K. Nedd8 on cullin: building an expressway to protein destruction. Oncogene 2004;23(11):1985–97. [PubMed: 15021886]
13. Wu K, Yamoah K, Dolios G, Gan-Erdene T, Tan P, Chen A, Lee CG, Wei N, Wilkinson KD, Wang R, Pan ZQ. DEN1 is a dual function protease capable of processing the C terminus of Nedd8 and deconjugating hyper-neddylated CUL1. J Biol Chem 2003;278(31):28882–91. [PubMed: 12759363]
14. Braumann C, Tangermann J, Jacobi CA, Muller JM, Dubiel W. Novel anti-angiogenic compounds for application in tumor therapy - COP9 signalosome-associated kinases as possible targets. Mini Rev Med Chem 2008;8(5):421–8. [PubMed: 18473931]
15. Hetfeld BK, Helfrich A, Kapelari B, Scheel H, Hofmann K, Guterman A, Glickman M, Schade R, Kloetzel PM, Dubiel W. The zinc finger of the CSN-associated deubiquitinating enzyme USP15 is essential to rescue the E3 ligase Rbx1. Curr Biol 2005;15(13):1217–21. [PubMed: 16005295]
16. Zhou C, Wee S, Rhee E, Naumann M, Dubiel W, Wolf DA. Fission yeast COP9/signalosome suppresses cullin activity through recruitment of the deubiquitylating enzyme Ubp12p. Mol Cell 2003;11(4):927–38. [PubMed: 12718879]
17. Wang X, Chen CF, Baker PR, Chen PL, Kaiser P, Huang L. Mass spectrometric characterization of the affinity-purified human 26S proteasome complex. Biochemistry 2007;46(11):3553–65. [PubMed: 17323924]
18. Wang X, Huang L. Identifying dynamic interactors of protein complexes by quantitative mass spectrometry. Mol Cell Proteomics 2008;7(1):46–57. [PubMed: 17934176]
19. Guerrero C, Milenkovic T, Przulj N, Kaiser P, Huang L. Characterization of the proteasome interaction network using a QTAX-based tag-team strategy and protein interaction network analysis. Proc Natl Acad Sci USA 2008;105(36):13333–38. [PubMed: 18757749]
20. Baker, PR.; Chalkley, RJ.; Wang, X.; Jen, N.; Huang, L. The Proceedings of 56th ASMS (American Society of Mass Spectrometry) Conference on Masss Spectrometry. American Society of Mass Spectrometry; Denver, CO: 2008. SILAC and iTRAQ Quantitation on an Orbitrap Using Protein Prospector.
21. Tagwerker C, Flick K, Cui M, Guerrero C, Dou Y, Auer B, Baldi P, Huang L, Kaiser P. A tandem affinity tag for two-step purification under fully denaturing conditions: application in ubiquitin profiling and protein complex identification combined with in vivocross-linking. Mol Cell Proteomics 2006;5(4):737–48. [PubMed: 16432255]
22. Guerrero C, Tagwerker C, Kaiser P, Huang L. An integrated mass spectrometry-based proteomic approach: quantitative analysis of tandem affinity-purified in vivo cross-linked protein complexes

(QTAX) to decipher the 26 S proteasome-interacting network. Mol Cell Proteomics 2006;5(2):366–78. [PubMed: 16284124]

23. Hetfeld BK, Bech-Otschir D, Dubiel W. Purification method of the COP9 signalosome from human erythrocytes. Methods Enzymol 2005;398:481–91. [PubMed: 16275352]
24. Menon S, Rubio V, Wang X, Deng XW, Wei N. Purification of the COP9 signalosome from porcine spleen, human cell lines, and Arabidopsis thaliana plants. Methods Enzymol 2005;398:468–81. [PubMed: 16275351]
25. Wei N, Deng XW. Characterization and purification of the mammalian COP9 complex, a conserved nuclear regulator initially identified as a repressor of photomorphogenesis in higher plants. Photochem Photobiol 1998;68(2):237–41. [PubMed: 9723217]
26. Yamoah K, Wu K, Pan ZQ. In vitro cleavage of Nedd8 from cullin 1 by COP9 signalosome and deneddylase 1. Methods Enzymol 2005;398:509–22. [PubMed: 16275355]
27. Polevoda B, Sherman F. Nalpha -terminal acetylation of eukaryotic proteins. J Biol Chem 2000;275 (47):36479–82. [PubMed: 11013267]
28. Sun Y, Wilson MP, Majerus PW. Inositol 1,3,4-trisphosphate 5/6-kinase associates with the COP9 signalosome by binding to CSN1. J Biol Chem 2002;277(48):45759–64. [PubMed: 12324474]
29. Uhle S, Medalia O, Waldron R, Dumdey R, Henklein P, Bech-Otschir D, Huang X, Berse M, Sperling J, Schade R, Dubiel W. Protein kinase CK2 and protein kinase D are associated with the COP9 signalosome. EMBO J 2003;22(6):1302–12. [PubMed: 12628923]
30. Beausoleil SA, Villen J, Gerber SA, Rush J, Gygi SP. A probability-based approach for high-throughput protein phosphorylation analysis and site localization. Nat Biotechnol 2006;24(10):1285–92. [PubMed: 16964243]
31. Inbal B, Shani G, Cohen O, Kissil JL, Kimchi A. Death-associated protein kinase-related protein 1, a novel serine/threonine kinase involved in apoptosis. Mol Cell Biol 2000;20(3):1044–54. [PubMed: 10629061]
32. Watabe-Uchida M, John KA, Janas JA, Newey SE, Van Aelst L. The Rac activator DOCK7 regulates neuronal polarity through local phosphorylation of stathmin/Op18. Neuron 2006;51(6):727–39. [PubMed: 16982419]
33. Lu H, Zong C, Wang Y, Young GW, Deng N, Souda P, Li X, Whitelegge J, Drews O, Yang PY, Ping P. Revealing the dynamics of 20S proteasome phosphoproteome: A combined CID and ETD approach. Mol Cell Proteomics. 2008[Online early access]. DOI: 10.1074/mcp.M80064-MCP200. Published Online: June 25, 2008
34. Tomoda K, Kubota Y, Arata Y, Mori S, Maeda M, Tanaka T, Yoshida M, Yoneda-Kato N, Kato JY. The cytoplasmic shuttling and subsequent degradation of p27Kip1 mediated by Jab1/CSN5 and the COP9 signalosome complex. J Biol Chem 2002;277(3):2302–10. [PubMed: 11704659]
35. Tsuge T, Matsui M, Wei N. The subunit 1 of the COP9 signalosome suppresses gene expression through its N-terminal domain and incorporates into the complex through the PCI domain. J Mol Biol 2001;305(1):1–9. [PubMed: 11114242]
36. Wang X, Kang D, Feng S, Serino G, Schwechheimer C, Wei N. CSN1 N-terminal-dependent activity is required for Arabidopsis development but not for Rub1/Nedd8 deconjugation of cullins: a structure-function study of CSN1 subunit of COP9 signalosome. Mol Biol Cell 2002;13(2):646–55. [PubMed: 11854419]
37. Jones J, Wu K, Yang Y, Guerrero C, Nillegoda N, Pan ZQ, Huang L. A targeted proteomic analysis of the ubiquitin-like modifier nedd8 and associated proteins. J Proteome Res 2008;7(3):1274–87. [PubMed: 18247557]
38. Bornstein G, Ganoth D, Hershko A. Regulation of neddylation and deneddylation of cullin1 in SCFSkp2 ubiquitin ligase by F-box protein and substrate. Proc Natl Acad Sci USA 2006;103(31): 11515–20. [PubMed: 16861300]
39. Jin J, Arias EE, Chen J, Harper JW, Walter JC. A family of diverse Cul4-Ddb1-interacting proteins includes Cdt2, which is required for S phase destruction of the replication factor Cdt1. Mol Cell 2006;23(5):709–21. [PubMed: 16949367]
40. Jin Y, Blue EK, Gallagher PJ. Control of death-associated protein kinase (DAPK) activity by phosphorylation and proteasomal degradation. J Biol Chem 2006;281(51):39033–40. [PubMed: 17056602]

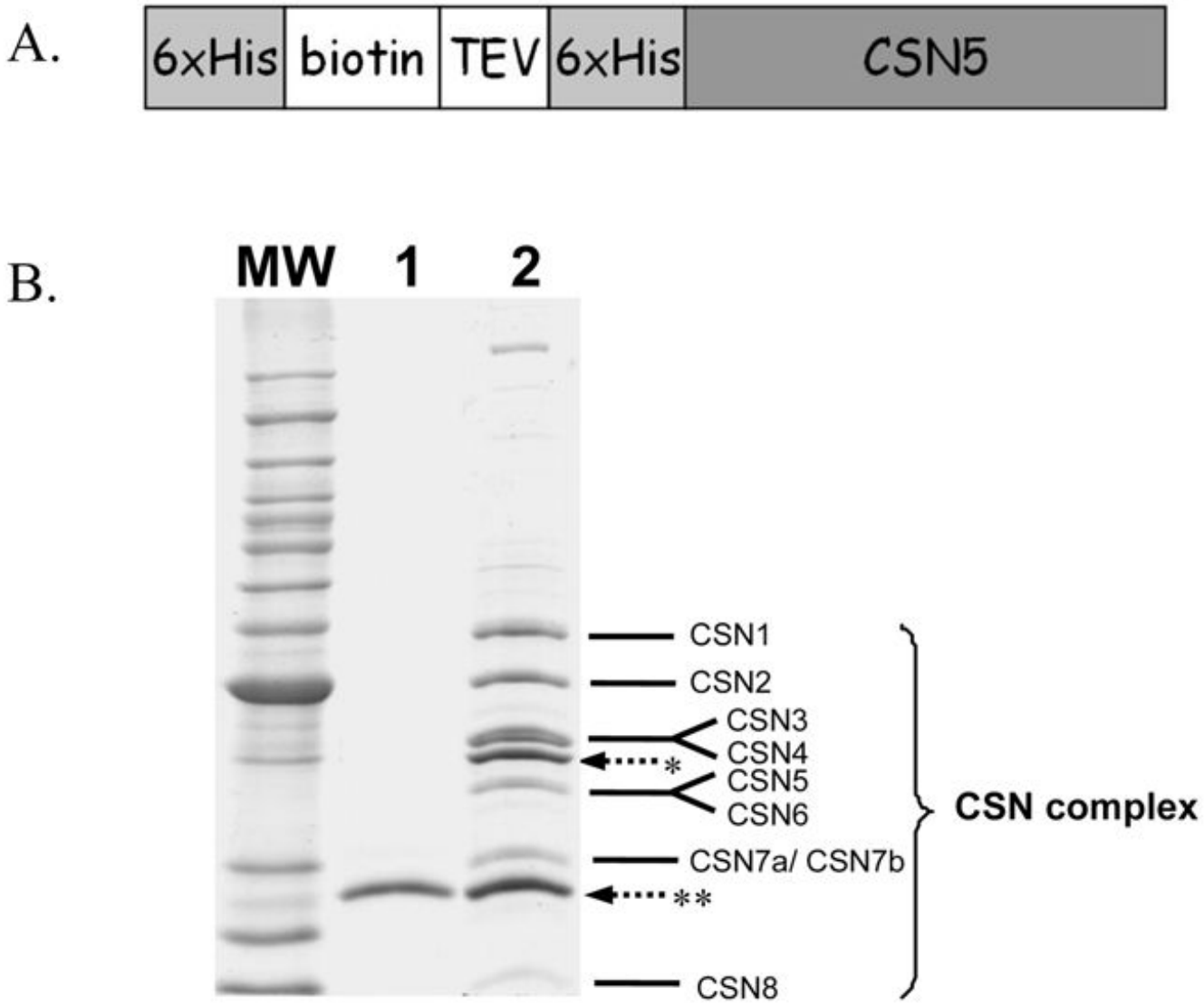

Figure 1.

Purification of the human CSN complex from $293^{HBTH\text{-}CSN5}$ cells. (A) Schematic representation of human CSN5 fused to the HBTH tag at its N-terminus; (B) 1D SDS-PAGE analysis of the purified CSN complex (lane 2) and the negative control (lane 1). The negative control was purified from 293^{HTBH} cells. (*) Tagged CSN5; (**) TEV protease.

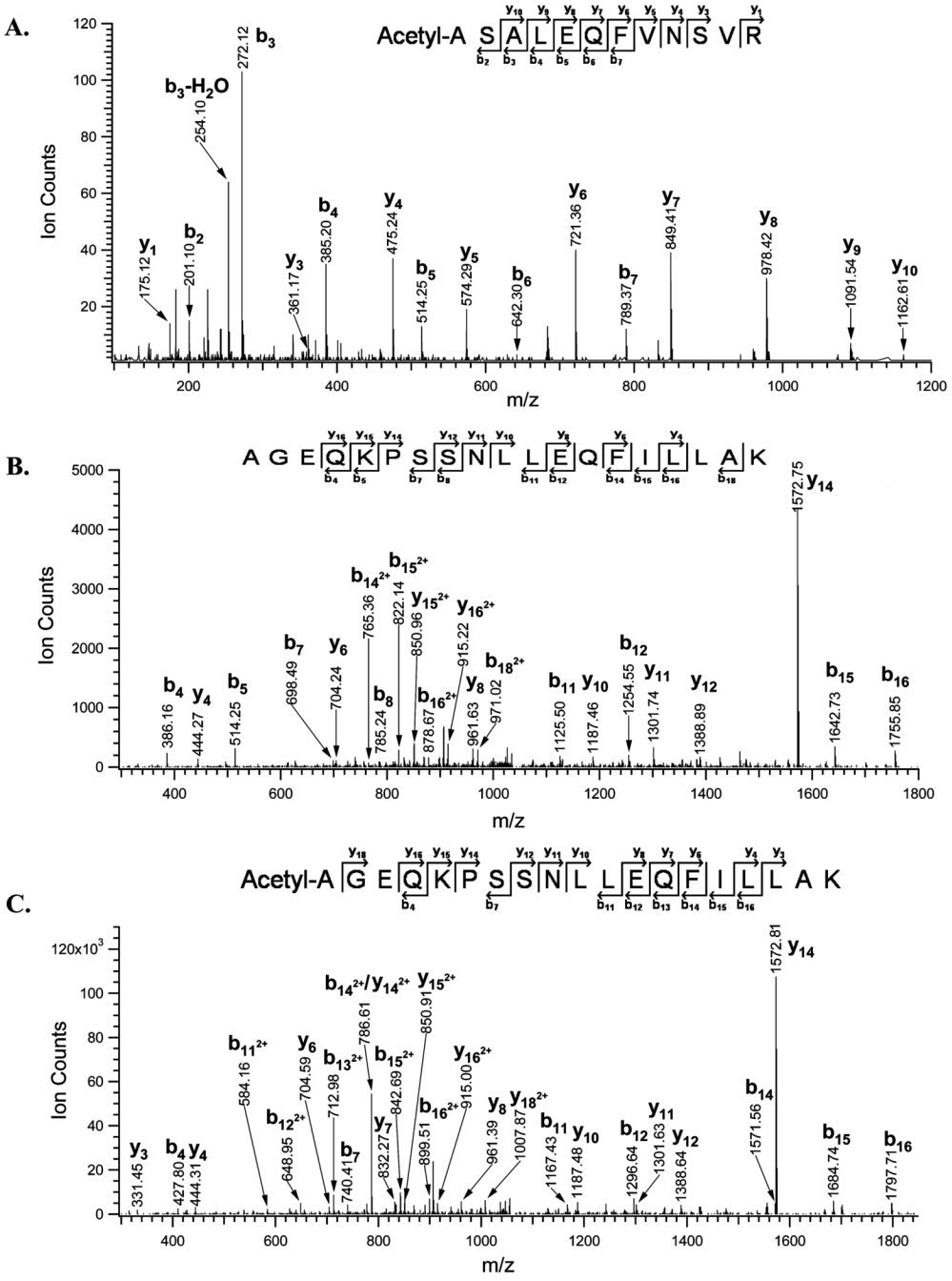

Figure 2.

ESI-MS/MS spectra of the selected N-terminal peptides identified for the CSN subunits: (A) a doubly charged tryptic peptide (MH_2^{2+} 681.85, Acetyl-ASALEQFVNSVR), matched to CSN3 subunit; (B) a doubly charged tryptic peptide (MH_2^{2+} 1043.58, AGEQKPSSNLLEQFILLAK); (C) a doubly charged tryptic peptide (MH_2^{2+} 1064.58, Acetyl-AGEQKPSSNLLEQFILLAK). The sequences in (B) and (C) matched to CSN7b subunit.

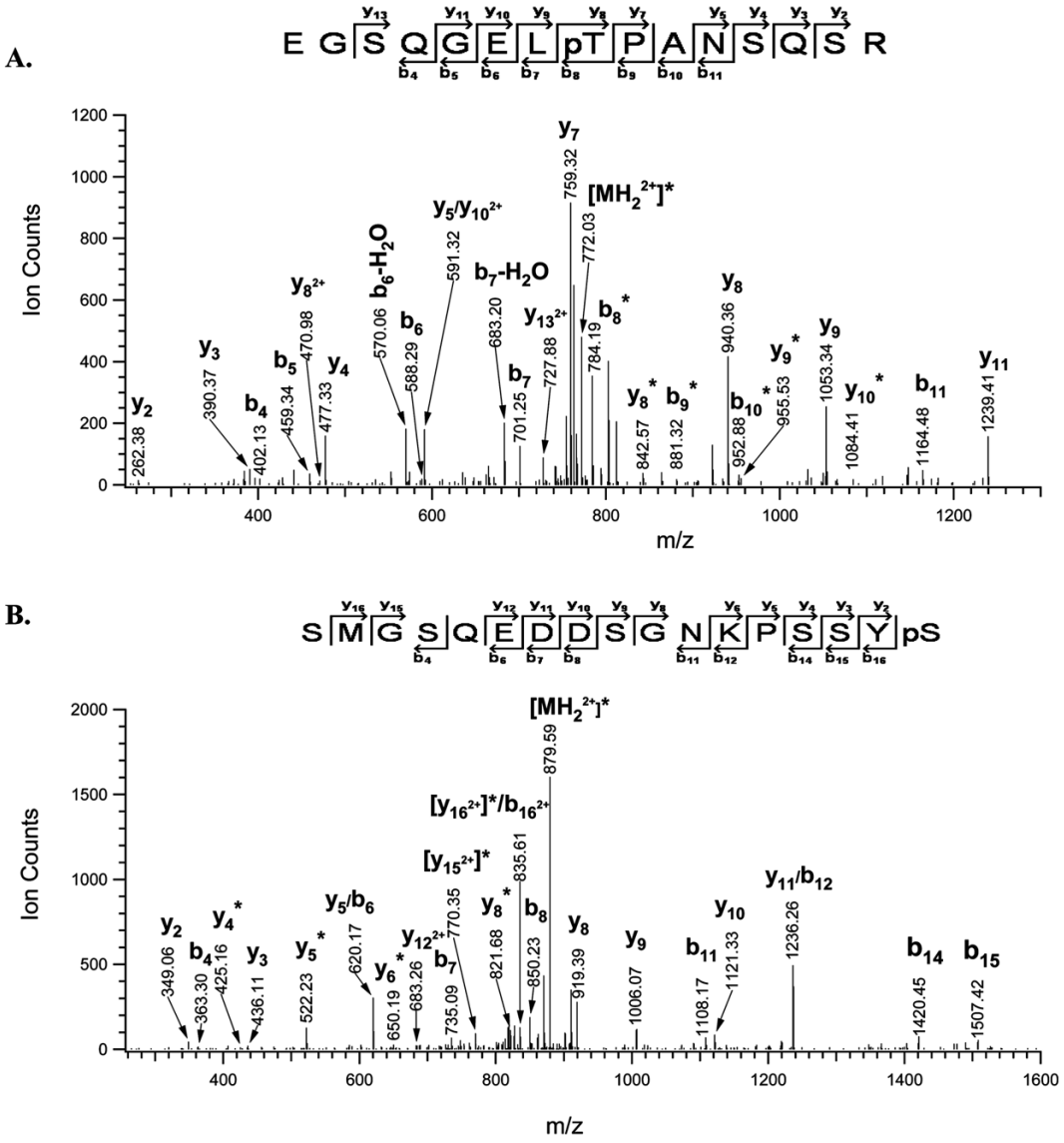

Figure 3.

Representative ESI-MS/MS spectra of phosphorylated peptides identified for CSN subunits: (A) a phosphorylated peptide (MH_2^{2+} 820.85, EGSQGELpTPANSQSR), matched to subunit CSN1; (B) a C-terminal phosphorylated peptide (MH_2^{2+} 928.34, SMGSQEDDSGNKPSSYpS), matched to CSN3. "*" Asterisk denotes ions after a single neutral loss ($-H_3PO_4$, −98 Da).

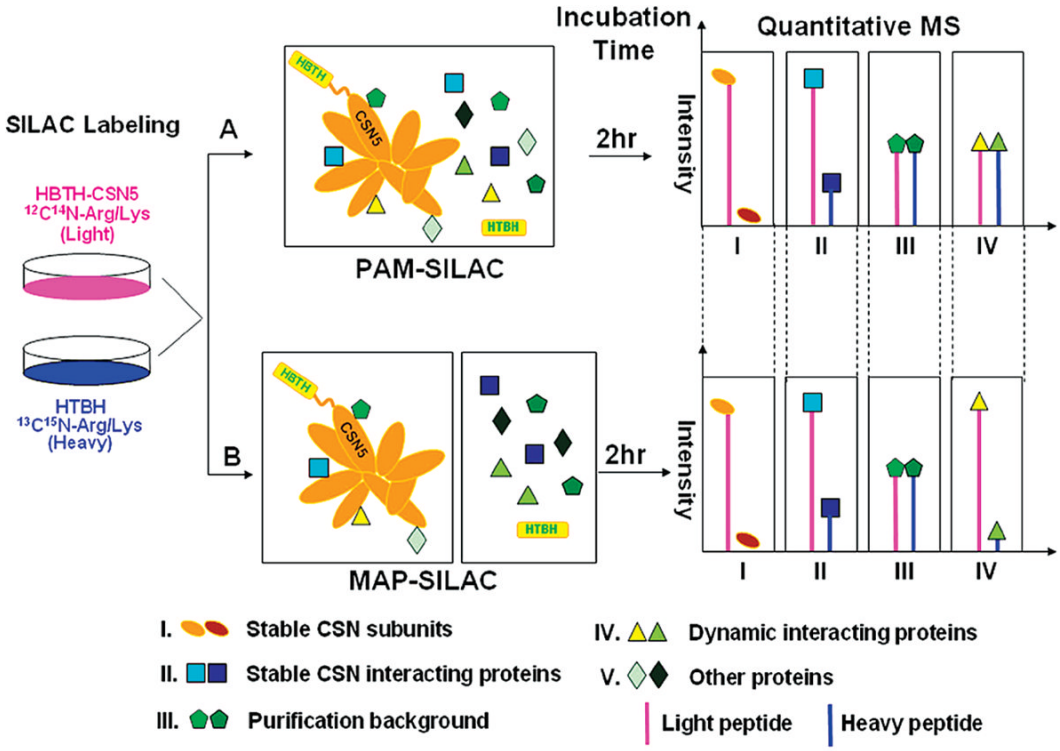

Figure 4.

SILAC-based strategies for identifying the dynamics of specific human CSN interacting proteins. The $293^{HBTH\text{-}CSN5}$ cells were grown in light (L) medium containing $^{12}C_6{}^{14}N_4$-Arg/$^{12}C_6{}^{14}N_2$-Lys (*pink*), whereas the 293^{HTBH} cells were grown in heavy (H) medium containing $^{13}C_6{}^{15}N_4$-Arg/$^{13}C_6{}^{15}N_2$-Lys (*blue*). Path (A) PAM-SILAC approach, in which protein purification was carried out after mixing of the two samples. Path (B) MAP-SILAC approach, in which protein purification was carried out separately prior to the mixing of the two samples.

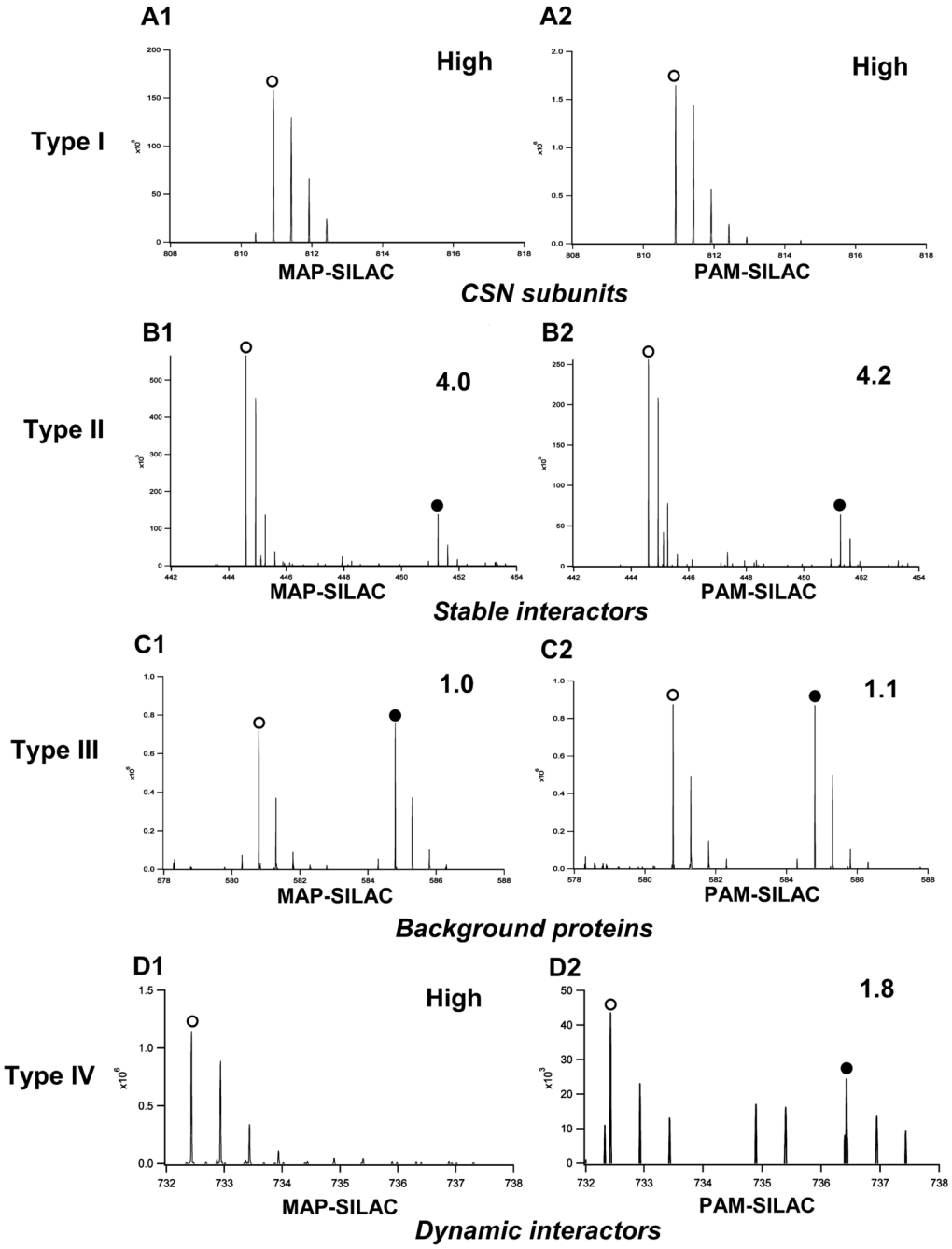

Figure 5.

Representative MS spectra of peptides derived from four different types of proteins identified in MAP-SILAC (A1–D1) and PAM-SILAC (A2–D2) experiments. The "○" and "●" represent the light and heavy forms of the peptide, respectively. The SILAC ratios (L/H) for each peptide are shown in the corresponding spectra. (A1–2) MS spectra of a tryptic peptide (MH_2^{2+} 810.92, VLELEGEKGEWGFK) matched to CSN2 subunit (Type I); (B1–2) MS spectra of a tryptic peptide (MH_3^{3+} 444.60, HRLPDLQAILR) matched to SPN90, a stable interacting protein (Type II); (C1–2) MS spectra of a tryptic peptide (MH_2^{2+} 580.80, SISLYYTGEK) matched to Nucleolin (Type III); (D1–2) MS spectra of a tryptic peptide (MH_2^{2+} 732.43, QLLGEHLTAILQK) matched to Cul-4A (Type IV).

Table 1

Summary of the CSN Subunits Identified Using Affinity Purification and LC-MS/MS

protein name	protein MW	accession number	no. of unique peptides	sequence coverage (%)	best disc. score	best expect val.
CSN 1	53372.5	Q13098	29	48.0	5.10	7.90×10^{-9}
CSN 2	51597.1	P61201	31	61.2	5.72	5.40×10^{-10}
CSN 3	47873.6	Q9UNS2	27	59.1	5.53	1.20×10^{-9}
CSN 4	46269.2	Q9BT78	32	68.7	4.49	1.00×10^{-7}
CSN 5	37579.2	Q92905	30	71.0	4.98	1.30×10^{-8}
CSN 6	36163.8	Q7L5N1	14	51.1	5.22	4.60×10^{-9}
CSN 7a	30276.9	Q9UBW8	11	44.7	4.89	1.90×10^{-8}
CSN 7b	29622.2	Q9H9Q2	8	34.8	3.89	1.40×10^{-6}
CSN 8	23225.8	Q99627	10	67.5	5.50	1.40×10^{-9}

Table 2

Identification of N-Terminal Peptides of Human CSN Subunits by LC-MS/MS

subunit name	accession number	*N-terminal Peptides of CSN Subunits in Protein Databases* *N-terminal Peptides of CSN Subunits Identified by MS/MS*
CSN1	Q13098	*MQIDVDPQEDPQNAPDVNYVVENPSLDLEQYAASYSGLMR*
		QIDVDPQEDPQNAPDVNYVVENPSLDLEQYAASYSGLMR
CSN3[a]	Q9UNS2	*MASALEQFVNSVR*
		Acetyl-ASALEQFVNSVR
CSN4	Q9BT78	*MAAAVRQDLAQLMNSSGSHK*
		Acetyl-AAAVRQDLAQLMNSSGSHK
CSN5[a]	Q92905	*MAASGSGMAQK*
		Acetyl-AASGSGMAQK
CSN5	Q92905	*MAASGSGMAQK*
		MAASGSGMAQK
CSN7a	Q9UBW8	*MSAEVKVTGQNQEQFLLLAK*
		Acetyl-SAEVKVTGQNQEQFLLLAK
CSN7b	Q9H9Q2	*MAGEQKPSSNLLEQFILLAK*
		Acetyl-AGEQKPSSNLLEQFILLAK
CSN7b	Q9H9Q2	*MAGEQKPSSNLLEQFILLAK*
		AGEQKPSSNLLEQFILLAK
CSN8	Q99627	*MPVAVMAESAFSFK*
		PVAVMAESAFSFK

[a]The N-termini of these subunits have been reported before.

Table 3

Summary of Phosphorylated Peptides of the CSN Subunits Identified by LC-MS/MS

accession number	phosphorylated peptide identified by MS/MS [a]	subunit name	possible kinases
Q13098	^{452}EGSQGELpTPANSQSR^{466}	CSN1	p38MAPK
Q13098	^{452}EGpSQGELTPANSQSR^{466}	CSN1	DNAPK
Q13098	^{452}EGSQGELpTPANpSQSR^{466}	CSN1	T459- p38MAPK
			S463-DNAPK
Q13098	^{442}NQIHVKpSPPR^{451}	CSN1	Cdk5
Q13098	^{442}NQIHVKSPPREGSQGELpTPANSQSR^{466}	CSN1	p38MAPK
Q13098	^{442}NQIHVKpSPPREGSQGELTPANSQSR^{466}	CSN1	Cdk5
Q13098	^{442}NQIHVKSPPREGpSQGELTPANSQSR^{466}	CSN1	DNAPK
Q13098	^{442}NQIHVKpSPPREGpSQGELTPANSQSR^{466}	CSN1	S448-cdk5
			S454-DNAPK
Q13098	^{448}SPPREGpSQGELTPANSQSR^{466}	CSN1	DNAPK
Q13098	^{448}pSPPREGSQGELTPANSQSR^{466}	CSN1	Cdk5
Q9UNS2	^{407}SMGSQEDDSGNKPSSYpS^{423}	CSN3	GSK3
Q9UNS2	^{407}SMGSQEDDSGNKPp(SS)YS^{423*}	CSN3	S420-Cdc2
			S421-DNAPK/GSK3
Q99627	^{166}KPVAGALDVpSFNK^{178}	CSN8	GSK3

[a] pS and pT represent phosphorylated serine and threonine, respectively. The potential kinases were determined based on the predicted results with the highest scores using NetPhosK1.0.

* The phosphorylation may occur on either Ser421 or Ser420.

Table 4

Identification of CSN Dynamic Interactors Using MAP-SILAC and PAM-SILAC Approaches[a]

	MAP-SILAC(1)			PAM-SILAC(1)			MAP-SILAC(2)			PAM-SILAC(2)			
acc	***n***	**avg**	**std**	***n***	**avg**	**std**	***n***	**avg**	**std**	***n***	**avg**	**std**	**protein name**
Q13620[b]	15	high	n/a	8	2.4	0.3	19	high	n/a	17	1.6	0.1	Cullin-4B
Q13619[b]	3	high	n/a	4	1.6	0.1	3	high	n/a	2	2.1	0.2	Cullin-4A
Q13618[b]	6	high	n/a	—	—	—	15	high	n/a	3	1.4	0.3	Cullin-3
Q13617[b]	5	high	n/a	—	—	—	12	high	n/a	1	1.4	—	Cullin-2
Q13616[b]	11	high	n/a	2	1.6	0.2	—	—	—	—	—	—	Cullin-1
Q16531[b]	19	high	n/a	8	2.9	0.7	33	high	n/a	13	2.2	0.3	DNA damage-binding protein 1
Q92466[b]	4	high	n/a	2	1.5	0.2	9	high	n/a	4	1.6	0.1	DNA damage-binding protein 2
Q6PJ61	3	high	n/a	2	1.6	0.3	—	—	—	3	1.2	0.2	F-box only protein 46
Q9P2K6	2	high	n/a	2	1.5	0.0	7	high	n/a	3	1.0	0.1	Kelch domain-containing protein 5
O15085	1	high	n/a	2	1.6	0.6	3	high	n/a	2	0.9	0.1	Rho guanine nucleotide exchange factor 11
P62877[b]	3	high	n/a	2	2.4	0.0	3	high	n/a	3	1.9	0.2	RING-box protein 1
O75970	20	15.4	3.9	10	2.3	0.6	13	16.0	5.4	7	1.7	0.4	Multiple PDZ domain protein
Q8N3R9	7	14.2	3.7	5	2.5	0.7	14	8.8	2.6	3	1.9	0.1	MAGUK p55 subfamily member 5
Q8NI35	2	13.9	2.5	6	2.7	0.7	1	13.0	n/a	1	2.5	—	InaD-like protein
Q9NUP9	2	9.1	1.2	2	2.2	0.6	1	8.2	—	2	1.2	0.1	Lin-7 homologue C
P35580	5	7.5	1.7	4	2.8	0.7	6	8.0	0.9	1	2.4	—	Myosin-10
Q5VUJ6	10	6.7	1.7	4	1.7	0.1	8	6.4	1.3	8	1.7	0.2	Leucine-rich repeat and calponin homology domain-containing protein 2
P53355	6	5.1	1.2	2	1.0	0.1	7	4.7	1.2	6	1.1	0.2	Death-associated protein kinase 1
O14974	14	3.3	0.4	9	0.7	0.1	9	2.9	0.6	2	0.9	0.1	Protein phosphatase 1 regulatory subunit 12A
Q9Y2D5	8	2.4	0.6	4	0.7	0.1	5	2.5	0.4	3	0.6	0.0	A-kinase anchor protein 2

[a] Note: Dynamic interactors are the proteins with MAP-SILAC ratios much higher than PAM-SILAC ratios (> 2-fold). *n*, number of unique peptides used for quantitation; avg, average value of SILAC ratios (L/H), high SILAC ratios indicate that the heavy labeled peaks of the peptide pairs were not detected; std, standard deviation of SILAC ratios in each experiment.

[b] Proteins are known to interact with CSN complex.